MANTECH Publications

Journal of Engineering Mathematics & Statistics
Volume 3, Issue 1, January-June 2019

Estimation of Maximum Water Levels Along East Coast of India due to Interaction of Storm Surge and Tide– Application to Cyclone Phailin (2013)

Farzana Hussain

Assistant Professor

Department of Mathematics

Huston Tillotson University, Austin, TX, USA

Corresponding Author's Email: *fhussain@htu.edu[1], farzanahsn@gmail.com[2]*

Abstract

Appropriate early warning systems for severe tropical cyclones and response networks are needed to ensure the safety of life and property along the coastal region. In this study a transformed coordinate boundary-fitted shallow water model is developed to predict the associated surge levels. Using appropriate transformations of independent coordinates, the curvilinear physical domain is transformed to a square one and also each island boundary transforms to a rectangle within this square domain. The vertically integrated shallow water equations are transformed to the new space domain and then the regular explicit finite difference scheme is used to solve the shallow water equations, where the problem domain is divided into 100× 131 grid points. The model is applied to compute the water levels due to astronomical tide and surges associated with Cyclone Phailin (2013) along the East coast of India. The computed results are found in good agreement with the observations.

Keywords: *Cyclone Phailin, Tropical Storms, Surge, Shallow water equations, Transformation of Coordinates, Bay of Bengal.*

AMS Subject Classifications: *35F30, 37M05, 65N06, 65N22, 65N50*

Page 22-41 © MANTECH PUBLICATIONS 2019. All Rights Reserved

INTRODUCTION

The Bay of Bengal, which borders India, Pakistan, Bangladesh, Myanmar, and Sri Lanka, has been home to the deadliest tropical cyclone disasters on Earth. A whopping 26 of the 35 deadliest tropical storms worldwide formed in the Bay of Bengal. That includes Cyclone Nargis, which struck Myanmar in 2008, killing an estimated 140,000 people. The Bhola Cyclone that struck Bangladesh in 1970 killed a staggering 300,000 to 500,000. Since that storm and several other deadly cyclones in this part of the world, scientists have worked to build robust early warning and response networks to ensure residents receive storm warnings and have safe places to go.

A tropical storm along with surges is the most destructive natural disaster for the coastal region of Bangladesh. The associated surge is more dangerous rather than the storm itself. Sometimes it may rise from 9 to 15 meters [24] and rushes towards the land, which causes severe damage to the life and property. The Bay of Bengal is surrounded by the coasts from all sides except in the south where there is open sea. The coastal geometry is curvilinear in nature and the bending of the coastline is very high moreover, there are many small and big islands in the offshore region. Various factors significantly increase the surge levels along the coast such as: shallowness of water, off-shore islands, bending of coastlines, oceanic bathymetry, low lying islands, huge discharge through the rivers etc. Also, the Head Bay of Bengal is a large tidal range area. Worst devastation may take place, if a storm approaches the coast at the time of high tide. Figure 1 shows the path of the cyclone Phailin and the cyclone affected areas of coastal region.

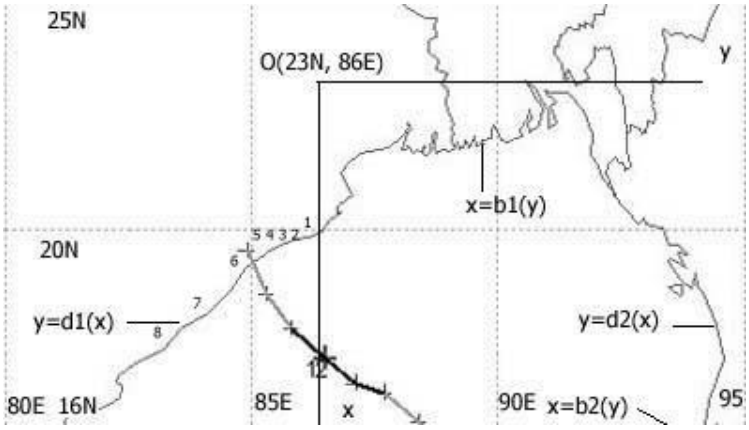


Figure 1 Path of Cyclone Phailin (the marked line), the analysis area and the locations at which results are presented

Page 22-41 © MANTECH PUBLICATIONS 2019. All Rights Reserved

Different procedures and techniques for numerical model development are studied for the Bay of Bengal [3 - 8, 14 -18, 20]. The representation of the coastal boundaries in those models was not so accurate and none of the off-shore islands are included in those models because very fine resolution could not be considered. If the grid size is not small, representation of the coastal and island boundaries are not accurate in a stair step models. Consideration of very fine resolution involves more computer memory and CPU time in the solution process and invites problem of numerical instability or complexity. In hydrodynamic models for coastal seas, bays, and estuaries the use of boundary-fitted curvilinear grids not only makes the model grids fit to the coastline, but also make the finite difference scheme simple and more accurate. In a boundary-fitted transformed coordinate model the curvilinear boundaries are transformed into straight ones, so that in the transformed domain regular finite difference technique can be used. [14] first used the partially boundary-fitted curvilinear grids in their transformed coordinate model for the east coast of India. The works [6, 7, 16, 17, 23, 26] were also based on representing the coasts by curvilinear boundaries and transformation of coordinates. But in those works two opposite boundaries were considered straight lines and none of them incorporated any offshore islands. The main difficulty in incorporating the islands was that, the whereabouts of the island boundaries were undetectable in the transformed domain. A model where a fine mesh numerical scheme for the Meghna estuary was nested into a coarse mesh scheme extending up to 15^0 N lat was developed in [22]. In the fine mesh scheme all the major islands were incorporated through proper stair step representation. The effect of presence of river on the surge development is discussed in [1] using boundary fitted stair step models. A storm surge for the Myanmar coast was developed in [11]. The expected total water levels for the coast of India, Pakistan are computed in [5, 12, 13]. In these works the east-west boundaries of the analysis area are considered as straight lines. [19, 20, 21] developed some models using nested numerical models. The complexity of the models lies in the matching of the boundary line of the fine mesh and curse mesh scheme within the domain. Recently [9, 10] developed a transformed coordinate shallow water model to simulate the water level along the Bangladesh coast. In that model the complete boundary of the physical domain is represented by four boundary-fitted curves or functions. Based on them, the four boundaries of islands are approximated by two generalized functions. Using mathematical transformations the physical domain becomes a square one and each island became a rectangle in the transformed domain.

Page 22-41 © MANTECH PUBLICATIONS 2019. All Rights Reserved

The present study attempts to develop an accurate surge forecasting model for the East coast of India based on transformation of coordinate. The vertically integrated shallow water equations are transformed into the new domain the regular explicit finite difference scheme with 100 × 131 grid points and 30s time step is used to solve the shallow water equations. In this model the major islands Bhola, Hatiya, Sandwip (of Bangladesh) are incorporated. The model is applied to compute the water levels due to tide, surge and their linear interaction associated with the storm Phailin (2013) along the East coast of India. Cyclone Phailin attacked the coast of India, the impact of these storm was severe - Seventeen people were killed in the state of Orissa and one person further south in the state of Andhra Pradesh. 600,000 people were left homeless in Orissa after the country's biggest cyclone in last 14 years. For the analysis and verification of the model, results are taken at 8 locations along the East coast of India. The locations are Bhubaneswar(1), Puri(2), Satapada(3), Ganjam(4), Gopalpur(5), Baruva(6), Shikakulam(7) and Visakhapatnam(8) (Figure 1). It is found that the model is quite capable to compute the tide and surge and the results are found reasonably accurate.

MATHEMATICAL FORMULATION OF THE PROBLEM

Boundary-Fitted Grids

A system of rectangular Cartesian coordinate is used in which the origin, O, is on the undisturbed level of sea surface. Ox points towards the south, Oy points towards the east and Oz is directed vertically upwards. The northern and southern coastal boundary of Bangladesh, is given by $x = \beta_1(y)$ and $x = \beta_2(y)$ respectively. The western and eastern coastal boundaries are at $y = \delta_1(x)$ and $y = \delta_2(x)$ respectively. This configuration is shown in Figure 1. It may be seen in the figure that the southern boundary $x = \beta_2(y)$ is taken as a straight line but this may be considered as a curve as well. Also it is to be noted that, the functions are not defined by explicit expressions, rather they are defined in tabular form. The boundary-fitted grids are generated through the following generalized functions:

The system of gridlines along $x = \beta_1(y)$ and $x = \beta_2(y)$ are given by the generalized function

$$x = \{(m-q)\,\beta_1(y) + q\,\beta_2(y)\}/m \qquad (1)$$

where m and q are constants and $0 \le q \le m$.

Page 22-41 © MANTECH PUBLICATIONS 2019. All Rights Reserved

The system of gridlines along $y = \delta_1(x)$ and $y = \delta_2(x)$ are given by the generalized function

$$y = \{(l - p)\,\delta_1(x) + p\,\delta_2(x)\}/l \qquad (2)$$

where l and p are constants and $0 \le p \le l$.

We note that, (1) reduces to $x = \beta_1(y)$ and $x = \beta_2(y)$ for $q = 0$ and $q = m$ respectively. Similarly, (2) reduces to $y = \delta_1(x)$ and $x = \delta_2(x)$ for $p = 0$ and $p = l$ respectively. By proper choice of q, m and p, l we can generate the boundary-fitted curvilinear grid lines.

Coordinate Transformation

A coordinate transformations based upon a new set of independent variables ξ, η, and t given by

$$\xi = \frac{x - \beta_1(y)}{\beta(y)}, \quad \beta(y) = \beta_2(y) - \beta_1(y) \qquad (3)$$

$$\eta = \frac{y - \delta_1(x)}{\delta(x)}, \quad \delta(x) = \delta_2(x) - \delta_1(x) \qquad (4)$$

These transform the physical curvilinear domain into the following rectangular one

$$0 \le \xi \le 1, \qquad 0 \le \eta \le 1$$

Also, the generalized functions given by (1) and (2) transforms to

$$\xi = q/m \qquad (5)$$

$$\eta = p/l \qquad (6)$$

The coastal boundary $x = \beta_1(y)$ or $\xi = 0$ are obtained for $q = 0$ and the open sea boundary $x = \beta_2(y)$ or $\xi = 1$ are obtained for $q = m$. Similarly, for $p = 0$, we have the western coastal boundary $y = \delta_1(x)$ or $\eta = 0$ and for $p = l$, we have the eastern coastal boundary $y = \delta_2(x)$ or $\eta = 1$. The appropriate choice of the constants m & l and the parameters q & p in (5) and (6) will generate the rectangular grid system in the transformed domain. Curvilinear boundaries of typical domain and the curvilinear grid system are shown in Fig. 2a. It may be noted that one of the boundaries is taken as straight line. In fact, it can be curved line as well. The corresponding boundaries and the rectangular grid system after the transformation are shown in Fig 2b.

Page 22-41 © MANTECH PUBLICATIONS 2019. All Rights Reserved

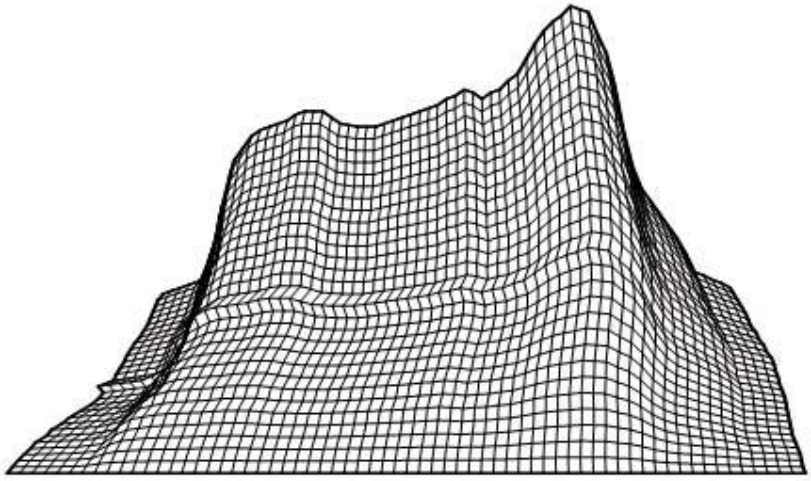


Figure 2a curvilinear boundaries and the curvilinear grid system

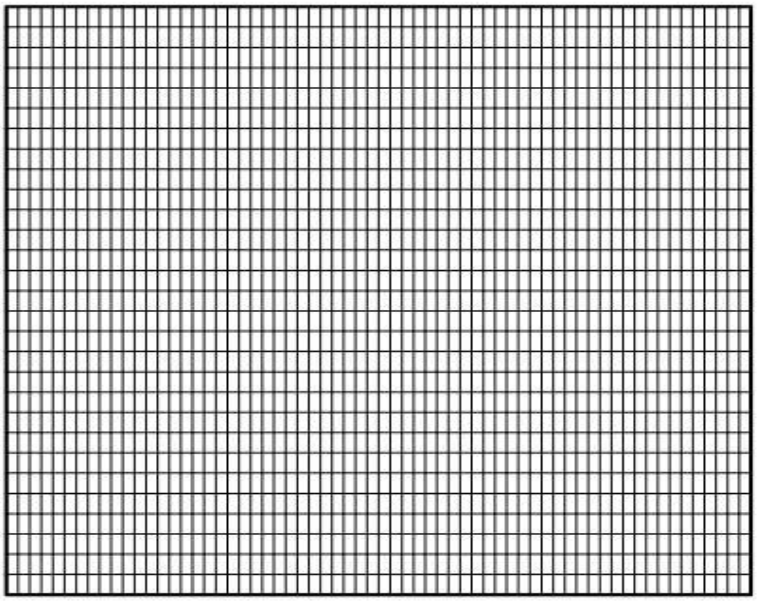


Figure 2b Boundaries and rectangular grid system in the transformed domain

Representation of Islands

The northern and southern boundaries of an island are given by (1) and the western and eastern boundaries are given by (2). Using the transformations (3) and (4) the boundaries of the island are given by (5) and (6). Thus two different values of q, say, q_1 and q_2 with $q_1 < q_2$ the northern and southern boundary of an island can be expressed by (5). Similarly, two different values of p, say, p_1 and p_2 with $p_1 < p_2$ the western and eastern boundary of the island will expressed by (6). Thus the transformed boundaries of an island are expressed as

Page 22-41 © MANTECH PUBLICATIONS 2019. All Rights Reserved

$$\xi = \frac{q_1}{m}, \quad \xi = \frac{q_2}{m}, \quad \eta = \frac{p_1}{l}, \quad \eta = \frac{p_2}{l} \tag{7}$$

Vertically Integrated Shallow Water Equations

The displaced position of the sea surface and the position of the sea floor are considered as $z = \zeta(x, y, t)$ and $z = -h(x, y)$ respectively. The vertically integrated shallow water equations given by [22] are

$$\frac{\partial \zeta}{\partial t} + \frac{\partial}{\partial x}\{(\zeta + h)\, u\} + \frac{\partial}{\partial y}\{(\zeta + h)\, v\} = 0 \tag{8}$$

$$\frac{\partial u}{\partial t} + u\frac{\partial u}{\partial x} + v\frac{\partial u}{\partial y} - f v = -g\frac{\partial \zeta}{\partial x} + \frac{\tau_x}{\{\rho(\zeta + h)\}} - \frac{c_f\, u(u^2 + v^2)^{1/2}}{(\zeta + h)} \tag{9}$$

$$\frac{\partial v}{\partial t} + u\frac{\partial v}{\partial x} + v\frac{\partial v}{\partial y} + f u = -g\frac{\partial \zeta}{\partial y} + \frac{\tau_y}{\{\rho(\zeta + h)\}} - \frac{c_f\, v(u^2 + v^2)^{1/2}}{(\zeta + h)} \tag{10}$$

The wind field over the physical domain is derived from the empirical formula given by

$$V_a = V_o(r/R)^{3/2} \quad for \quad r \le R$$
$$= V_o(R/r)^{1/2} \quad for \quad r > R \tag{11}$$

Radial and tangential components of wind stress are derived by

$$(\tau_r, \tau_\theta) = C_D\, \rho_a (u_a^2 + v_a^2)^{1/2}(u_a, v_a) \tag{12}$$

τ_x and τ_y, the x and y component of wind stress in (9) and (10) are derived from τ_r and τ_θ.

The Boundary Conditions

The boundary conditions used in this model following [17] are given by

$$u - v\frac{d}{dy}(\beta_1) = 0 \quad \text{at } x = \beta_1(y) \tag{13}$$

$$u - v\frac{d}{dy}(\beta_2) = (g/h)^{1/2}\zeta \quad \text{at } x = \beta_2(y) \tag{14a}$$

$$v - u\frac{d}{dx}(\delta_1) = 0 \quad \text{at } y = \delta_1(x) \tag{15}$$

$$v - u\frac{d}{dx}(\delta_2) = 0 \quad \text{at } y = \delta_2(x) \tag{16}$$

Page 22-41 © MANTECH PUBLICATIONS 2019. All Rights Reserved

For generating tide in the basin the southern open sea boundary condition is taken as

$$u - v\frac{d}{dy}(\beta_2) = (g/h)^{1/2}\,\zeta - 2(g/h)^{1/2}\ a\ Sin[(2\pi t)/T + \varphi] \text{ at } x = \beta_2(y) \qquad (14b)$$

where a and φ denote respectively the prescribed amplitude and phase of the tidal force and T is the tidal period.

Governing Equations and Boundary Conditions in the Transformed Domain

For the transformation (3) and (4), we have

$$\frac{\partial}{\partial x} \equiv \frac{\partial \xi}{\partial x}\frac{\partial}{\partial \xi} + \frac{\partial \eta}{\partial x}\frac{\partial}{\partial \eta}$$

$$\frac{\partial}{\partial y} \equiv \frac{\partial \xi}{\partial y}\frac{\partial}{\partial \xi} + \frac{\partial \eta}{\partial y}\frac{\partial}{\partial \eta}$$

Using these operators in (8) – (10), we have the following transformed equations:

$$\frac{\partial \zeta}{\partial t} + \frac{\partial}{\partial \xi}\{(\zeta + h)U\} + \frac{\partial}{\partial \eta}\{(\zeta + h)V\} = 0 \qquad (17)$$

$$\frac{\partial u}{\partial t} + U\frac{\partial u}{\partial \xi} + V\frac{\partial u}{\partial \eta} - f\,v = -g\left[\frac{\partial \zeta}{\partial \xi}\frac{1}{\beta} - \frac{\partial \zeta}{\partial \eta}\frac{\{(\delta_1)_x + \eta\,\delta_x\}}{\delta}\right]$$
$$+ \frac{\tau_x}{\rho(\zeta + h)} - \frac{c_f\,u\,(u^2 + v^2)^{1/2}}{\zeta + h} \qquad (18)$$

$$\frac{\partial v}{\partial t} + U\frac{\partial v}{\partial \xi} + V\frac{\partial v}{\partial \eta} + f\,u = -g\left[\frac{\partial \zeta}{\partial \eta}\frac{1}{\delta} - \frac{\partial \zeta}{\partial \xi}\frac{\{(\beta_1)_y + \xi\,\beta_y\}}{\beta}\right]$$
$$+ \frac{\tau_y}{\rho(\zeta + h)} - \frac{c_f\,v\,(u^2 + v^2)^{1/2}}{\zeta + h} \qquad (19)$$

where

$$U = u\frac{\partial \xi}{\partial x} + v\frac{\partial \xi}{\partial y} = \frac{u - \{(\beta_1)_y + \xi\,\beta_y\}v}{\beta} \qquad (20)$$

$$V = u\frac{\partial \eta}{\partial x} + v\frac{\partial \eta}{\partial y} = \frac{v - \{(\delta_1)_x + \eta\,\delta_x\}u}{\delta} \qquad (21)$$

The boundary condition (13) - (16) transform to

$$U = 0 \qquad \text{at } \xi = 0 \qquad (22)$$

$$\beta U - (g/h)^{1/2}\zeta = 0 \qquad \text{at } \xi = 1 \qquad (23a)$$

$$\beta U - (g/h)^{1/2}\zeta = -2(g/h)^{1/2}\ a\ Sin[(2\pi t)/T + \varphi] \qquad \text{at } \xi = 1 \qquad (23b)$$

Page 22-41 © MANTECH PUBLICATIONS 2019. All Rights Reserved

$V = 0$ at $\eta = 0$ (24)

$V = 0$ at $\eta = 1$ (25)

The normal component of velocity vanishes at each boundary of an island. Thus from (7), the boundary conditions for an island are given by

$U = 0 \quad at \quad \xi = q_1 / m \quad \& \quad \xi = q_2 / m$ (26)

$V = 0 \quad at \quad \eta = p_1 / l \quad \& \quad \eta = p_2 / l$ (27)

Numerical Set up of the Model

The curvilinear grid system in the physical domain is generated through (1) and (2). In the transformed domain the corresponding rectangular grid system is generated through (5) and (6) with appropriate choice of m, l, q, and p. The curvilinear grid system is shown in Fig 2a and the corresponding rectangular grid system is shown in Fig 2b.

Let us define discrete coordinate points in the transformed domain by

$\xi = \xi_i = (i - 1)\, \Delta\xi, \; i = 1, 2, \ldots, n_i$

$\eta = \eta_j = (j - 1)\, \Delta\eta, \; j = 1, 2, \ldots, n_j$

A sequence of time instant is given by

$t = t_k = k\, \Delta t, \; k = 1, 2, 3, \ldots$

In the computational domain we use staggered grid in which there are three distinct types of computational points. With i even and j even, the point is a ζ- point at which ζ is computed. If i is odd and j is even, the point is a u- point at which u is computed. If i is even and j is odd, the point is a v- point at which v is computed. We choose n_i (= 100) to be even so that at the southern open boundary there are ζ- points and v- points only. Similarly we choose n_j (= 129) to be odd thus ensuring that there are only ζ- points and v- points at the eastern and western boundaries. The coastal boundary is approximated either along the nearest odd grid line (i = odd) given by (1) so that we have only u- points on this part of the boundary or along the nearest odd grid line (j = odd) given by (2) so that we have only v- points along that part of the boundary. The island boundaries are also approximated in the same manner. Thus, the boundaries of the coast and of the islands are represented by such a system of stair steps that, at each segment (stair) there exists only that component of velocity which is normal to the

Page 22-41 © MANTECH PUBLICATIONS 2019. All Rights Reserved

segment. This is done in order to ensure the vanishing of the normal component of velocity at the boundaries in the numerical scheme.

The governing equations (17) – (19) and the boundary conditions (22) – (27) are discretized by finite difference (forward in time and central in space) and are solved by conditionally stable semi- implicit method using staggered grid as mentioned earlier. For numerical stability, the velocity components in (18) and (19) are modeled in a semi-implicit manner. For example, in the last term of (18) the time discretization of $\tilde{u}(u^2 + v^2)$ is done as $\tilde{u}^{k+1}(u^2 + v^2)^k$ where the superscript k and k +1 denote values at the present and advanced time levels respectively. Moreover, the CFL criterion has been followed in order to ensure the stability of the numerical scheme. Along the closed boundary, the normal component of the velocity is considered as zero, and this is easily achieved through appropriate stair step representation as mentioned earlier.

The initial value of ζ, u, and v are taken as zero. The time step is taken as 30s that ensures stability of the numerical scheme. In the solution process, a uniform value of 0.0026 for the friction coefficient (C_f) and 0.0028 for the drag coefficient (C_D) are considered throughout the physical domain.

In this model the analysis area is extended from 80^0 E to 95^0 E along the East coast of India, Bangladesh and Mayanmar. The open sea boundary is situated along 16^0 N (Fig. 1). The east-west extent of the analysis area varies between $x = \beta_1(y)$ and $x = \beta_2(y)$ and the north-south extent varies between $y = \delta_1(x)$ and $y = \delta_2(x)$. The analysis area has been divided to 100 x 129 grid points. Thus in the north-south direction $\Delta x = \beta(y)/n_j$ while in the east-west direction $\Delta y = \delta(x)/ n_i$. In the transformed domain we consider $\Delta\xi = 1.0/(n_i - 1)$, and $\Delta\eta = 1.0/(n_j - 1)$ so that $q_i = (i - 1)\,\Delta\xi = \xi_i$ and $p_j = (j - 1)\,\Delta\eta = \eta_j$.

The offshore region of Bay of Bengal is full of big and small islands with a high density around the Meghna estuary. In this study it is possible to incorporate the small islands by considering very fine resolution in the numerical scheme; we consider the major islands Bhola, Hatiya, Sandwip, Moheshkhali more accurately.

Page 22-41 © MANTECH PUBLICATIONS 2019. All Rights Reserved

RESULTS AND DISCUSSIONS

Analysis of the Computed Surge Response

The model is applied to compute the water levels due to tide and surge associated with Cyclone Phailin that hit the East coast of India recently with maximum sustained anti-clock wise circulatory wind velocities of 260 km/h (72.22 m/s). Table.1 gives the history of the above-mentioned storm, the data of which was received from the Website of Weather Unisys (Figure 1).

Table 1 History of the chosen storm Phailin (2013)

Storm of 2013 Phailin				
Date	Hour	Lat.	Long.	Wind
1009	00	13.20	93.40	35
1009	06	13.40	92.80	40
1009	12	13.70	92.20	40
1009	18	14.10	91.60	50
1010	00	14.40	91.30	55
1010	06	14.90	91.00	65
1010	12	15.40	90.30	100
1010	18	15.60	89.40	125
1011	00	15.80	88.80	135
1011	06	16.10	88.40	135
1011	12	16.70	87.70	140
1011	18	16.90	87.10	140
1012	00	17.40	86.50	140
1012	06	18.00	85.80	130
1012	12	18.70	85.30	120
1012	18	19.60	84.90	100

Cyclone ‘Phailin’ **was the** biggest cyclone in last14 years **that hit the Indian coast** and was also favorable for high surge due to both wind intensity and path of its movement. The system was first noted as a tropical depression on October 4, 2013 within the Gulf of Thailand. During the next day Phailin intensified rapidly and became a very severe cyclonic storm on October 10, equivalent to a category 1 hurricane. On October 11, the system became equivalent to a category 5 hurricane with diameter about 500 km, central pressure of 918mb before it started to weaken during the next day as it approached the Indian state of Odisha. It made landfall later that day, near Gopalpur in Odisha coast at around 2130 IST (1600 UTC) with sustained wind 200 km/h. It subsequently weakened over land as a result of frictional

Page 22-41 © MANTECH PUBLICATIONS 2019. All Rights Reserved

forces, before it was last noted on October 14. Authorities had predicted a storm surge of at least 3m (10ft) that was expected to cause extensive damage.

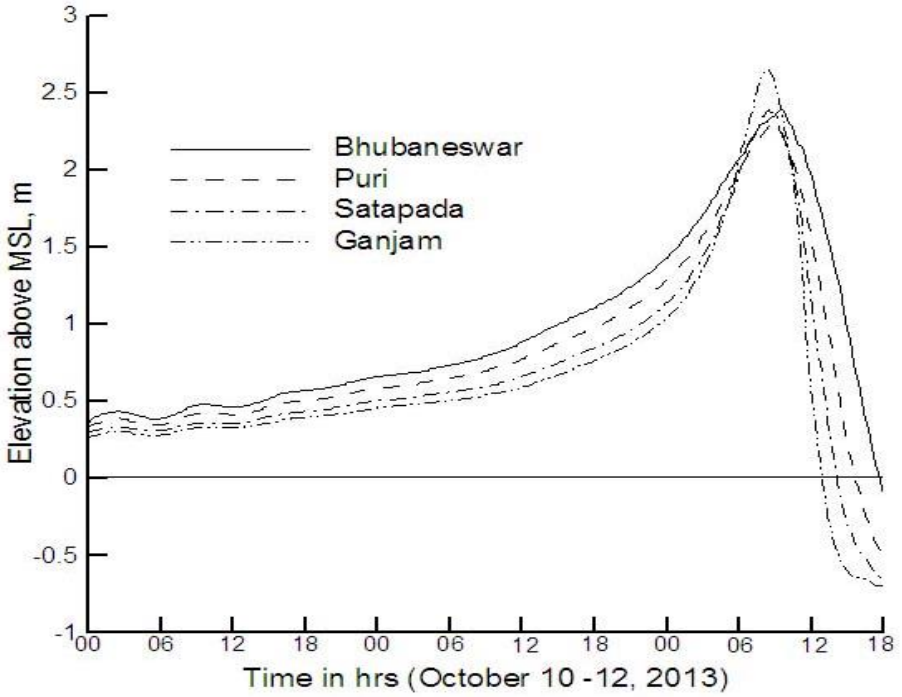


Figure 3a Computed time series of surge levels at different coastal locations

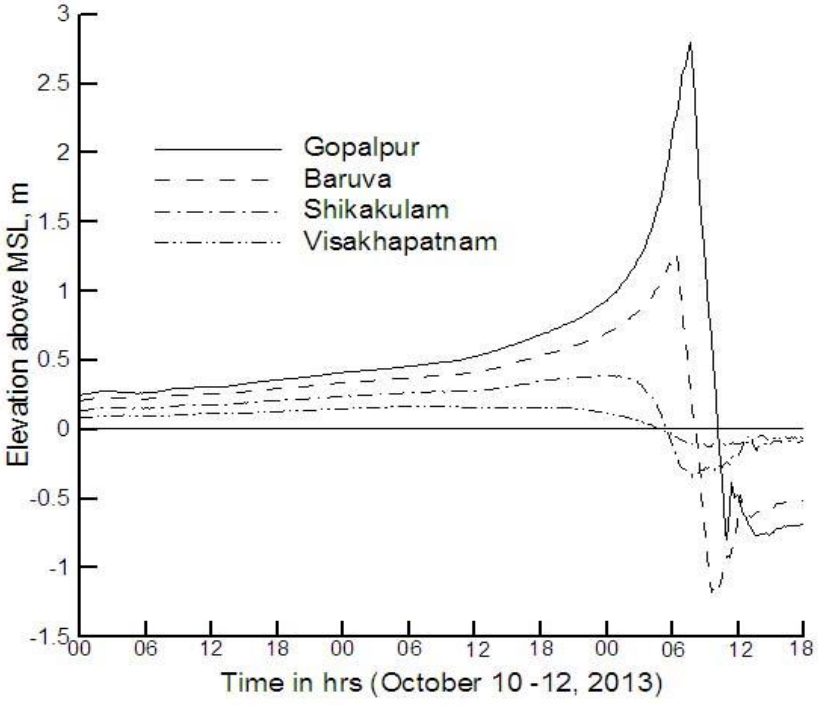


Figure 3b Computed time series of surge levels at different coastal locations

Page 22-41 © MANTECH PUBLICATIONS 2019. All Rights Reserved

Figure 3a, b depicts the computed surge levels associated with 'Phailin' at different coastal locations. It may be observed in the figures that, the surge level is increasing with time as the storm approaches towards the coast and finally there is recession. At Baruva a strong recession is occurred around 06:00 UTC of 12th October, earlier than in any other locations and before the landfall time. The recession takes place due to backwash of water from the shore towards the sea. In fact, Baruva is situated along left (west) of the storm path and so the direction of the anti-clock wise circulatory wind becomes northerly (i.e. towards the sea) at Baruva before the storm reaches the coast and thus driving the water towards the sea. The recession reaches up to -1.25 m approximately at 11:00 UTC of 15th November. It may be noticed that the recession at other places began later than Baruva (Figs. 3a, 3b). Thus the beginning of recession delays as we proceed towards east as is expected. At every location, the peak surge is attaining before the land falls time of the storm. This is expected, as the circulatory wind intensity is highest along the coast when the storm reaches near the coast. According to a storm surge analysis report by the Indian Meteorological Department (IMD), there was 3 to 3.5 meters surge along the coastal regions between Baruva and Bhubaneswar. Thus, the computed surge heights are almost identical with the report. The same information is also found in the website of Wikipedia [30].

Analysis of the Computed Tide and Tide-Surge Interaction

We know, the astronomical tide is a continuous process in the sea, the surge due to tropical storms always interacts with the astronomical tide. So the pure tidal oscillation is the initial dynamical condition for interaction of tide and surge. The tide is generated in the model through the south open boundary condition (23b) with appropriate values of a, T, and φ in absence of wind stress. It is observed that, though there is variation in the tidal period in the head Bay of Bengal, the average period is approximately of M_2 tide and so we choose T = 12.4 hrs. By trial it is found that $\varphi = 0$ is a good choice for head Bay region. The information of the amplitude a along the southern boundary is not available. We have chosen $a = 0.6\ m$ to test the response of the model along the coastal belt (Figure 4a, b). It is found that response is exactly sinusoidal with the same period (12.4 hrs), which is expected. About the phase it may be seen that Bhubaneswar, Puri, Satapada, Ganjam are in the same phase of tidal oscillation. This is because of the fact that, they are very close to each other. But Visakhapatnam is far away from these coastal points having different tidal phase. Hence providing appropriate

Page 22-41 © MANTECH PUBLICATIONS 2019. All Rights Reserved

values of the amplitude *a* along the southern open sea boundary condition the model can be used to generate the actual tidal oscillation in the whole basin.

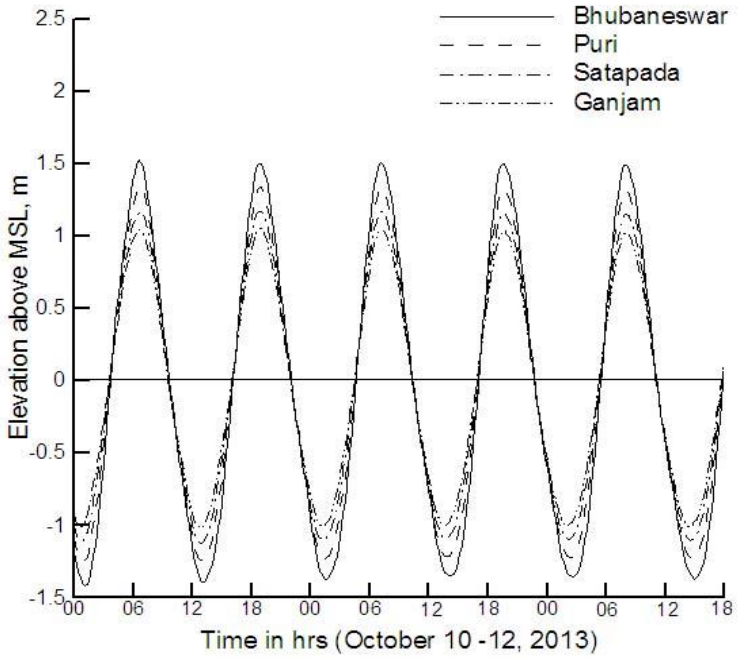


Figure 4a Computed tidal oscillations at different coastal locations

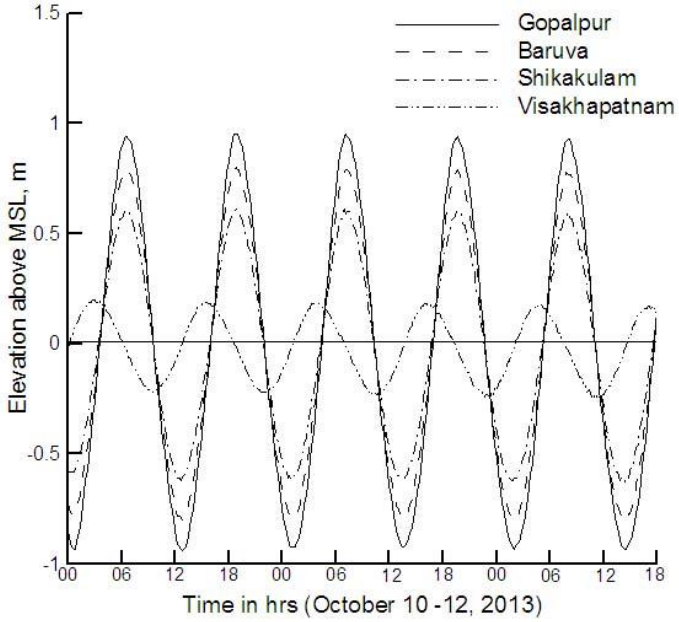


Figure 4b Computed tidal oscillations at different coastal locations

Page 22-41 © MANTECH PUBLICATIONS 2019. All Rights Reserved

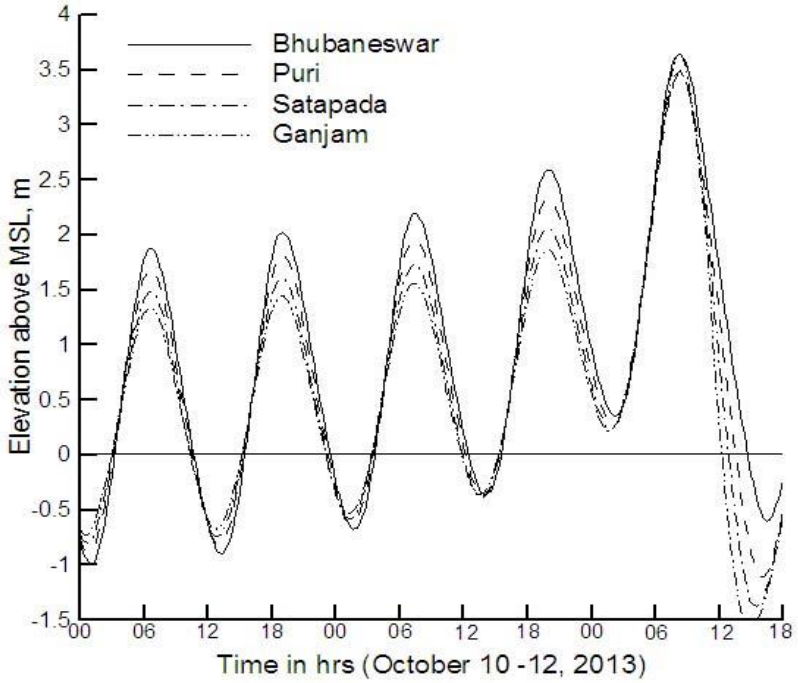


Figure 5 a Linear interaction of computed tide and computed surge at different coastal locations

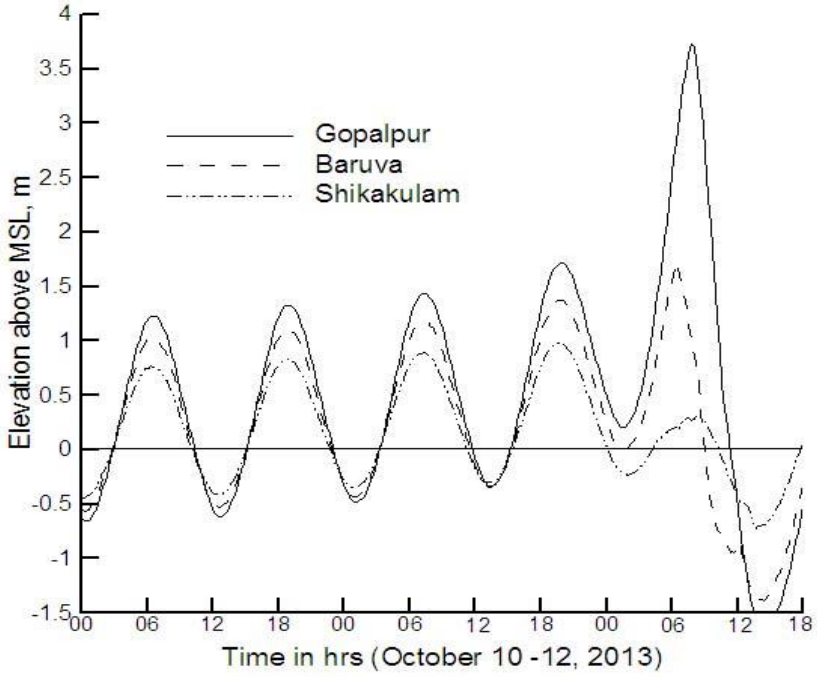


Figure 5b Linear interaction of computed tide and computed surge at different coastal locations

Page 22-41 © MANTECH PUBLICATIONS 2019. All Rights Reserved

Figure 5a and b shows the linear interaction of tide and surge at different coastal locations. At each location, because of weak wind the surge response is less when the storm is away from the coast and the total water level is dominated by tidal oscillation. On the other hand, because of very strong wind the water level is dominated by surge when the storm approaches the cost. The maximum water level occurred at Gopalpur is 3.6 m.

Finally, Figure 6a shows the Contours (in meters) of equal sea surface elevation for peak surge along the Bay of Bengal. Figure 6b shows the Contours (in meters) of equal sea surface elevation for surge level at the time of landfall. It is seen that, at the time of landfall the surge levels along the left side of the storm path is negative and along the right side of the storm path is positive. This is attributed to the anti circulatory wind velocity at that time.

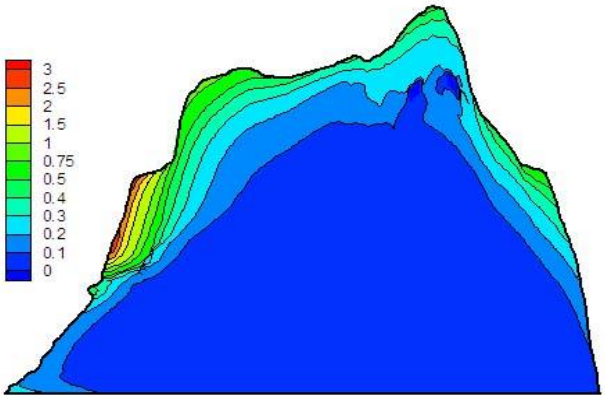


Fig 6a Contours (in meters) of equal sea surface elevation for peak surge

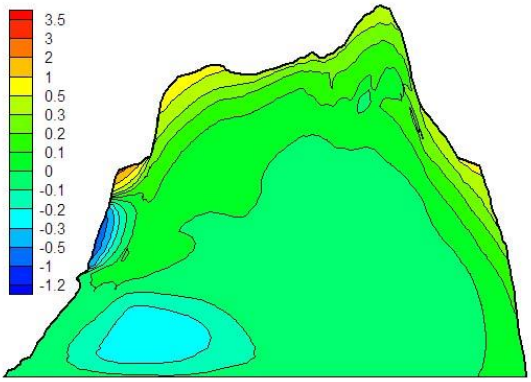


Fig 6b Contours (in meters) of equal sea surface elevation at the time of landfall

Page 22-41 © MANTECH PUBLICATIONS 2019. All Rights Reserved

CONCLUSION

In this study a numerical model based on transformation of coordinates is developed to compute the tide and surge levels associated with a storm along the East coast of India. This shallow water model can be applied to compute water levels along the Coast of Bangladesh and Myanmar also. The model is also applicable for any bay or estuary or even in any confined lake. The model is capable of incorporating the bending of coastline and island boundaries with a considerable accuracy. The model results are found to be in good agreement with the observations.

REFERENCES

I. Agnihotri Neetu, Chittibabu, P., Indu Jain, Rao, A. D., Dube, S. K., Sinha P. C.: A Bay-River Coupled Model for storm surge prediction along the Andhra coast of India. Natural Hazards. **39**, 83-101 (2006).

II. Bao, X.W., Yan, J., Sun, W. X: A three-dimensional tidal model in boundary-fitted curvilinear grids. Estuarine, Coastal and Shelf Science, **50**, 775 – 788 (2000).

III. Das, P. K: Prediction model for storm surges in the Bay of Bengal, Nature, **239**, 211-213 (1972).

IV. Das, P. K., Sinha M. C., Balasubrahmanyam, V: Storm surges in the Bay of Bengal, Quart J. Roy. Met. Soc. **100**, 437- 449 (1974).

V. Dube, S. K., Indu Jain, Rao, A. D., T. S. Murty: Storm surge modelling for the Bay of Bengal and Arabian sea. Natural Hazards. **51**, 3-27 (2009).

VI. Dube, S. K., Sinha, P. C., Roy, G. D.: The numerical simulation of storm surges along the Bangladesh coast. *Dyn. Atms. Oceans.* **9**, 121-133 (1985).

VII. Dube S. K., Sinha, P. C., Roy, and G. D.: The numerical simulation of storm surges in Bangladesh using a bay-river coupled model. Coastal Engineering. **10**, 85-101 (1986).

VIII. Flierl, G. R., Robinson, A. R.: Deadly surges in the Bay of Bengal: Dynamics and

Page 22-41 © MANTECH PUBLICATIONS 2019. All Rights Reserved

storm tide tables. Nature, **239**, 213-215 (1972).

IX. Hussain Farzana: A Transformed Coordinates Shallow water Model for the Head of the Bay of Bengal using Boundary-Fitted Curvilinear Grids. East Asian Journal on Applied Mathematics, **3(1)**, 27-47 (2013).

X. Hussain Farzana: A Boundary-Fitted Shallow Water Model To Simulate Tide And Surge For The Head Bay Of Bengal – Application To Cyclone Sidr (2007) And Aila (2009). International Journal of Mathematical Modelling & Computations. **3(4), 275-297,** (2013)

XI. Jain Indu, Neetu Agnihotri, Chittibabu, P., Rao, A. D., Dube, S. K., Sinha P. C.: Simulation of storm surges along Myanmar coast Using a location specific Numerical model. Natural Hazards. **39**, 71-82 (2006).

XII. Jain Indu, Chittibabu, P., Neetu Agnihotri, Dube, S. K., Rao, A. D., Sinha P. C.: Numerical Storm surge model for India and Pakistan. Natural Hazards. **42**, 67-73 (2007)

XIII. Jain Indu, Rao, A. D., Dube, S. K., V. Jitendra: Computation of Expected total water levels along the east coast of India. Journal of coastal research. **26(4),** 681-687 (2010).

XIV. Johns B. Dube, S. K. Mohanti, U. C., Sinha, P. C.: Numerical simulation of surge generated by the 1977 Andhra cyclone. Quart. J. Roy. Soc. London. **107**, 919-934 (1981).

XV. Johns B., Ali, A.: The numerical modeling of storm surges in the Bay of Bengal. Quart. J. Roy. Met. Soc., **106**, 1-18 (1980).

XVI. Johnson, B. H.: Numerical modeling of estuarine hydrodynamics on a boundary fitted coordinate system. Numerical Grid Generation (Thompson, J., ed.) Elsevier. 419 - 436 (1982)

Page 22-41 © MANTECH PUBLICATIONS 2019. All Rights Reserved

XVII. Johns B., Dube, S. K., Mohanti, U. C., Sinha, P. C.: The simulation of continuously deforming lateral boundary in problems involving the shallow water equations. Computers and Fluids. **10**, 105-116 (1982) .

XVIII. Johns, B., Rao, A. D., Dube, S. K., Sinha P. C.: Numerical modeling of tide-surges interaction in the Bay of Bengal. Phil. Trans. R. Soc. of London A313, 507-535 (1985).

XIX. Rahman M. M., Hoque A., Paul G. C. and Alam M. J.: Nested Numerical Schemes to Incorporate Bending Coastline and Islands of Bangladesh and Prediction of Water Levels due to Surge, Asian Journal of Mathematics and Statics, **4(1)**, 21 -32 (2011).

XX. Rahman M. M., Hoque A., Paul G. C.: A Shallow Water Model Water Model for the coast of Bangladesh and Applied to Estimate water levels for AILA. Journal of Applied Sciences, 11(24), 3821 -3829 (2011).

XXI. Rahman M. M., Hoque A., Paul G. C.: A Cyclone Induced Storm Surge forecasting Model for the coast of Bangladesh with Application to the Cyclone Sidr. International Journal of Mathematical Modelling and Computations. **1(2)**, 77 -86, (2011).

XXII. Roy, G. D.: Estimation of expected maximum possible water level along the Meghna estuary using a tide and surge interaction model. Environment International. **21(5)**, 671- 677 (1995).

XXIII. Roy, G. D.: Some aspects of storm surges along the coast of Bangladesh. Ganith (J. Bangladesh Math. Soc. **6(1),** 1- 8, (1985).

XXIV. Roy G. D.: Inclusion of offshore islands in transformed coordinates shallow water model along the coast of Bangladesh. Environment international. **25(1),** 67- 74, (1999).

XXV. Roy G. D., Humayun Kabir, A. B. M., Mandal, M. M., Haque, M. Z.: Polar coordinate shallow water storm surge model for the coast of Bangladesh. Dyn. Atms.

Page 22-41 © MANTECH PUBLICATIONS 2019. All Rights Reserved

Oceans, **29**, 397- 413, (1999).

XXVI. Sinha, P. C., S. K. Dube, and G. D. Roy: Numerical simulation of storm surges in Bangladesh using a multi-level model. Int. J. for Num. methods in fluids. **6**, 305-311, (1986).

XXVII. Sheng, Y. P.: On modelling three- dimensional estuarine and marine hydrodynamics. Three- dimensional Models of Marine and Estuarine Dynamics (Nihoul J. C.J, ed.) Elsevier Oceanography Series. **45**, 35 – 54 (1989)

XXVIII. Spaulding, M. L.: A vertical averaged circulation model using boundary-fitted coordinates. Journal of Physical Oceanography, **14**, 973 – 982 (1984)

XXIX. Thompson, J.F., Frank, C., Thames, F.C., Mastin, C.W.: Automatic numerical generation of body-fitted curvilinear systems for tied containing any number of arbitrary two-dimensional bodies. Journal of Computational Physics, **15**, 229-319 (1974)

XXX. http://en.wikipedia.org/wiki/Cyclone_Phailin

Page 22-41 © MANTECH PUBLICATIONS 2019. All Rights Reserved